Effect of Air Bubble Injection on the Flow Near a Rotary Device

N.M. Nouri[1] and A. Sarreshtehdari[2]
Applied Hydrodynamics Laboratory, Mech. Eng. Dep't.
Univ. of Science and Tech. of Iran.

ABSTRACT
In the work, modification of wall shear stress due to air bubble injection on a rotary apparatus was experimentally investigated. In this device, water flow field causes a rotary motion of hub by shear forces. Injected air bubbles cross the near wall region of the hub surface and affect its rotary behavior (in constant water flow rates). Void fraction increase leads to decrease of rotational velocity provided by the flow shear stresses. In high-void fractions, the hub motion stops completely. The amount of skin friction reduction was estimated by measurement of hub rotational velocity. Rotational velocity decrease, due to bubble injection leads to the reduction of wall shear stress in all range of water flow rates. More than 90 percent of rotational velocity reduction was achieved in maximum void fraction. This result expresses the significant reduction of shear stress on the rotary hub. The considerable amount of skin friction reduction obtained in this special test case indicates the effectiveness of gas bubbles injection on skin friction reduction in some rotary parts for special applications.

Key Words: Skin Friction Reduction, Microbubble, Drag Reduction

تأثیر تزریق حباب هوا در جریان مجاور یک قطعه استوانه‌ای چرخان

نوروز محمد نوری و علی سررشته داری
آزمایشگاه تحقیقاتی هیدرودینامیک کاربردی، دانشکده مهندسی مکانیک، دانشگاه علم وصنعت ایران

(تاریخ دریافت: ۱۳۸۶/۰۹/۱۰؛ تاریخ پذیرش: ۱۳۸۷/۰۷/۱۰)

چکیده
مطالعات تجربی کاهش تنش برشی به کمک تزریق میکروحباب در این پژوهش مورد بررسی قرار گرفته است. در این راستا، حباب های تولید شده توسط دستگاه مولد میکروحباب وارد جریان گذرنده از کنار توپی چرخان می‌شود که تنها توسط مؤلفه برشی جریان عبوری به حرکت در می‌آید و سرعت چرخشی آن که تابعی از ویژگی‌های جریان، از جمله سرعت مماسی است، نشان دهندهٔ میزان تنش برشی اعمال شده از طرف سیال به جسم است. آزمایش های مختلف نشان می‌دهد که سرعت چرخشی‌ای که متناسب با اصطکاک پوسته‌ای است، با سرعت جریان، در محدوده آزمایش‌های انجام شده در این تحقیق، رابطه مستقیم دارد. کاهش قابل توجهی در سرعت چرخشی در اثر تزریق میکروب‌ها در تمامی محدوده‌های عدد رینولدز آزمایش شده ملاحظه می‌شود. نتایج به دست آمده کاهش سرعت چرخشی تا ۹۰ درصد را با استفاده از این روش نشان می‌دهد و مقدار کم کسر حجمی گاز در آزمایش‌ها امکان پذیری کاربرد عملی از این شیوه را تأیید می‌کند.

واژه‌های کلیدی: کاهش اصطکاک پوسته‌ای، میکروحباب، کاهش درگ

1- Assistant Professor: mnouri@iust.ac.ir
2- PhD Student (Corresponding Author): sarreshtedari@iust.ac.ir

1- Introduction

Microbubbles are used for various industrial applications, such as water treatment and fishery cultivated shells [1]. They also have properties well-suited for physiological and physiochemical purposes [2]. The reduction of skin friction of ships is one of the most important applications of microbubbles with diameters smaller than several tens of microns. This type of drag reduction is particularly important for maritime transportation applications, since 80 percent of total drag in a large ship is due to skin friction [3]. Moreover, this technique of reducing skin friction reduction is an environmentally friendly method, compared to other methods such as polymer drag [4]. McCormick and Bhattacharyya [5] towed a 1.22-m long, fully submerged hull in a towing tank. They created small bubbles around the hull using electrolysis and found out that by using this technique. Drag could be reduced significantly Some researchers use electrolysis for microbubble generation, especially for laboratory purposes (e.g. [6]); but this technique is not useful for industrial research and applications [7-8]. Some microbubble generators use a combination of methods, such as depressurization of air-saturated water, bubble break-up by shear force, and cavitation. Generation of a homogeneous distribution of small air bubbles for microbubble drag reduction experiments is indispensable. For this purpose, sintered metal filters, comprised of porous materials with tiny holes, play a vital role. Latorre et al. [7] injected microbubbles to the vertical sides of a high-speed model with a non-wetting coating and achieved overall drag reduction of 4 to 11 percent. Sanders et al. [8] performed experiments on a 12.9m-long, hydraulically smooth, flat plate on which a near-zero-pressure-gradient flat plate turbulent boundary layer was generated. Their results showed that the liquid layer next to the surface limits the amount and persistence of bubble drag reduction, and this phenomenon may be active even when buoyancy pushes bubbles toward the test surface. The results also showed that the amount of drag reduction strongly depends on the near-wall void fraction and the importance of bubble buoyancy. Chanson [9] investigated air injection in open-channel flows. The results exhibit smaller friction losses than non-aerated flows. It is shown that the drag reduction process is linked to the presence of an air-bubble concentration boundary layer near the channel bottom. Fujiwara et al. [10] conducted an experimental study in vertical, upward-driven, bubbly pipe flow with void fractions of 0.5 and 1.0 percent to explain the effect of dispersed bubble size on turbulence modification. The high concentration of bubbles in the vicinity of the wall induced a reduction of the fluctuation velocity intensity of the liquid.

Murai et al. [11] experimentally investigated bubble distributions organized in a vertical Taylor-Couette flow and demonstrated that the wall shear stress decreases as bubbles are injected in all of the tested range of Reynolds numbers from 600 to 4500. In the bubble-injection drag reduction, as many researchers [12-14] have emphasized, the size of bubbles is an essential issue, microbubble size should be the smaller or in an order of smallest eddies length scales in turbulent flow to be effective on the turbulent boundary layer. On the other hand, Shen et al. [15] indicated that the drag reduction by microbubbles is strongly related to the injected gas volumetric flow rate and the static pressure in the boundary layer, but is essentially independent of the size of the microbubbles. Villafuerte & Hassan [12] generated hydrogen and oxygen microbubbles by electrolysis and achieved drag reductions up to 40 percent. Wu et al. [13] used a porous medium to generate microbubbles, and their experiments in pipe showed more drag reduction (26 percent) when using 1μm porous medium than while using 10μm porous medium at the same flow velocity (around 23 percent). Recently, the bubble-size dependency of the average skin friction in the intermediate bubble size condition was observed by injecting bubbles of size 2 to 90 μm, approximately, to the boundary layer thickness in a horizontal turbulent channel flow [14]. In these experiments, the local skin friction significantly decreased in the rear part of individual large bubbles, and rapidly increased after the bubble's rear interface passed.

Although some hypotheses have been presented regarding the mechanisms playing a role in bubble-injection drag reduction, such as transport effects associated with mixture density, turbulence energy extraction associated with breakup, diminished turbulence production and bubble deformation, none of them have yet been confirmed [16]. In order to clarify the mechanism of drag reduction caused by microbubbles, Kitagawa et al. [17] experimentally investigated the turbulence structure of a horizontal channel flow with microbubbles. They proposed a new system which simultaneously measures the liquid phase and the dispersed bubbles, based on a combination of particle tracking velocimetry (PTV), laser-induced fluorescence (LIF) and the shadow image technique (SIT). Using these techniques, the turbulence characteristics of the flow field, including measurements for both phases, and bubble effects on the turbulence were quantified.

Although modeling microbubble motion is a challenging task because of the vague mechanism of microbubble drag reduction (MBDR),

Considerable effort has been made into this. [16-19]. Lu et al. [16] investigated the effect of a few relatively large bubbles injected near the walls on the wall drag in the "minimum turbulent channel" by direct numerical simulation (DNS), and detected significant reduction of wall drag by suppressing the streamwise vorticity due to deformable bubbles. Ferrante and Elghobashi [18] used numerical simulations for a microbubble-laden, spatially developing turbulent boundary layer and compared the amount of skin friction reduction due to the presence of the bubbles for two Reynolds numbers. Their results show that increasing the Reynolds number decreases the percentage of drag reduction. Although direct numerical simulation of the microbubble turbulent boundary layer provides insight into the physical phenomena responsible for drag reduction, it is not currently feasible to use it for practical purposes. thus other computational methods have been used for bubble modeling. Kunz et al. [19] introduced a new model for MBDR based on a eulerian two-fluid model. Emphasis is placed on the modeling strategies required to capture measured volume fraction, bubble size, and bubble velocity distribution, as well as skin friction drag reduction. Also, a 2-D, single-phase, computational fluid dynamics (CFD) model of microbubble-laden flow over a flat plate was used to assess the role of mixture density variation in microbubble drag reduction [20]. Studies indicated that the simple mixture-density variation effect plays one of the major roles in the microbubble drag reduction phenomenon.

In the present research, variation of skin friction by bubble injection was investigated on the rotational hub in various void fractions. In this apparatus, water enters the device via six diagonal nozzles and mixes with air coming from small holes at the bottom of the device. The experiments demonstrate a direct relation between the rotational velocity of hub and skin friction, and more than 80 percent skin friction reduction was achieved.

2- Experimental Setup

The apparatus used for generating bubbles is a symmetric, cylindrical device including a central rotary hub and an external shell. Fig. **1** illustrates a section of this device. Liquid and gas are injected into the device and exit circumferentially through an outlet. The geometrical shapes of the region through which liquid-gas mixture passes and the angle of the diagonal water holes are deliberately selected to maximize the rotational velocity of the liquid-gas mixture. Furthermore, two bearings have been used to support the central hub and facilitate the tendency of rotation. In this model, bubbles are broken in three different stages. At the first stage, they are broken due to injection through the holes. During the second stage, rotational flow makes the bubbles pass a longer trajectory. At this stage, high-velocity flow and long-distance movement separate the bubbles and prevent them from merging with each other. On the other side, the turbulent shear stress breaks them continuously. Lastly or finally or others like these, large shear stresses caused by the narrow outlet break the bubbles for the final step. The region through which the liquid-gas mixture passes is purposefully shaped to maximize the rotational velocity of gas-fluid mixture. Angles of the diagonal nozzle for water injection are selected so that the tangential velocity of the entering water is much more than radial velocity in order to force the central hub to rotate, Fig. **2**.

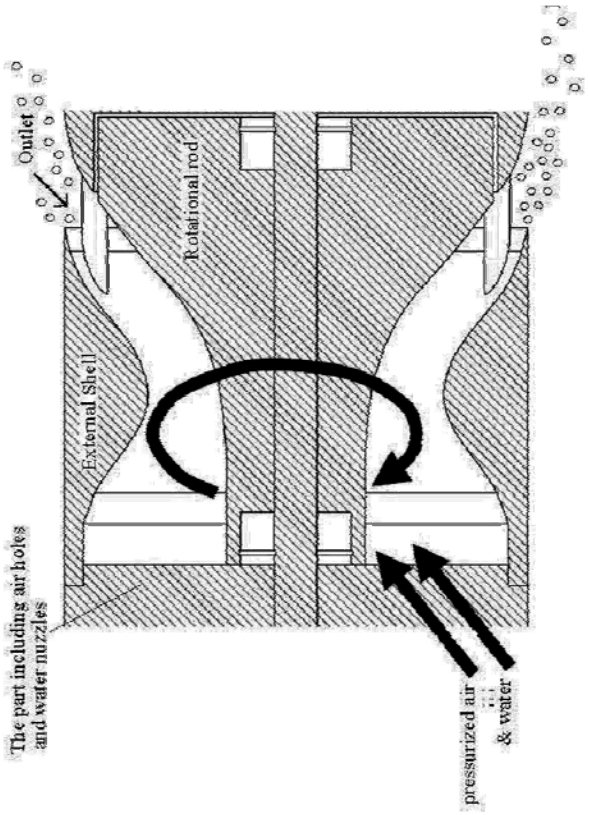

Fig. (1): Section of axisymmetric device including a central rotary hub and an external fixed shell.

Furthermore, two bearings have been used to support the central hub and promote the tendency to rotate. In order to obtain an optimum geometry for the area that the liquid-gas mixture passes through, numerical simulations were used to simulate a single-phase flow for some different geometries proposed during design procedure.

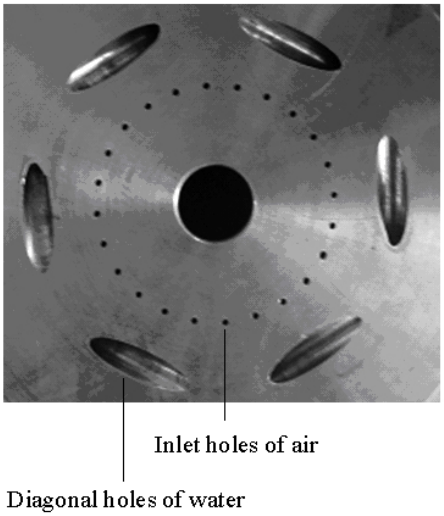

Fig. (2): Straight and diagonal nozzles through which air and water are injected to the device.

Rotational velocity in the region, turbulent kinetic energy and the trajectories at which water elements travel were considered as the effective parameters for optimum geometry selection. The more turbulent kinetic energy and longer trajectories of fluid elements would be cause bubbles size diminish. Figure **3** shows the experiment set-up. The bubble generator device was installed at the bottom of a cylindrical tank with a depth of $1.5m$ and volume of $1.6m^3$. The tank has four transparent windows for lighting and taking images. Water flow enters the nozzles via a centrifugal pump. Flow rate is measured by a flow meter and is adjusted by a valve. A compressor with maximum pressure of 500 kpa is used to provide and inject pressurized air into straight air holes of the device. The flow rate is measured by a calibrated rotameter and adjusted by a valve. The pressure of the injected air was adjusted to 110 ± 5 kpa in all experiments. When the bubbles were ejected, the apparatus gradually rose up. At the top of the tank, a membrane (E) was used to separate air bubbles from water in order to recycle the water to the flow meter and the pump.

3- Test Procedures

Shear stress between water flow and rotary hub surface is the only excitation force which obliges the hub to rotate. Shen et al. showed that water impurities, e.g. salt and other surfactant solutions, affect microbubble size distribution and skin friction changes consequently; therefore in these tests, water purity is constant in the all of the tests [15]. Evaluation of the effects of bubble injection on the variation of skin friction was observed by measuring the angular velocity of the central hub. Experimental results demonstrate the direct relation between changing the skin friction and the angular velocity of hub. Therefore, a set of experiments were done by changing the flow rate of water and air. During each test, the angular velocity of the rotary hub and the flow rates of water and air were recorded in order to calculate the void fractions of each test and also to evaluate the variation of skin friction effects. In addition, a sufficient time gap was considered between each two consecutive tests in order that all the parameters, such as air flow rate and water flow rate, were invariant.

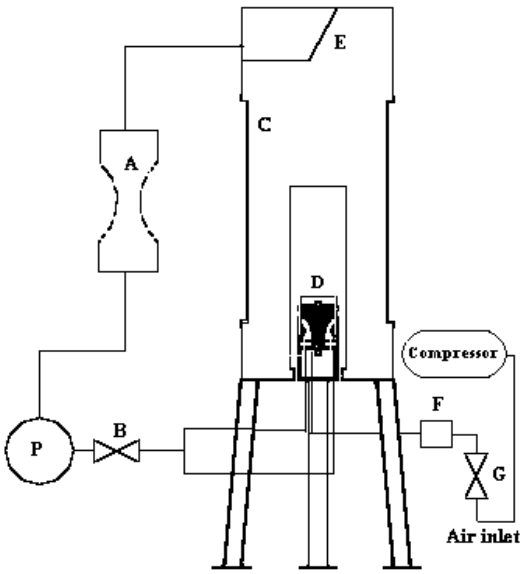

Fig. (3): Experimental setup (A: Water flow meter, B: Water flow control valve, C: Water tank, D: Testing device, E: Membrane bubble separator, P: Pump, F: The rotameter, G: Air flow control valve).

4- Results and Discussion

All conducted tests were carried out in turbulent flows with a volumetric water flow rate of about $4.7 lit/\sec$. Also, the quantity of the air injected into the flow was changed from zero to $0.15 lit/s$ in order to determine the effect of void fraction variations on skin friction. The average void fraction in the test section is estimated by:

$$\alpha = \frac{Q_a}{Q_w + Q_a}, \qquad (1)$$

where, Q_a and Q_w are air flow rate and water flow rate, respectively. The relative error of air flow rate measurement is 0.001 according to the air flow meter characteristics, and that of water flow rate is 0.1. Therefore, the measurement uncertainty of the average void fraction is 0.01. Compressed air with inlet pressure of approximately 110 kpa entered the bottom of the apparatus for generation of microbubbles while water flow circulated in the setup. The above-mentioned water and air flow

rates were adjusted by two valves for a void fraction from 0 to 3.1. Microbubbles of sizes smaller than 500 micron in diameter were produced either in minimum or maximum air flow rates as shown in Fig's. **4**-**5**. Bubbles' sizes were determined using an image processing method [21].

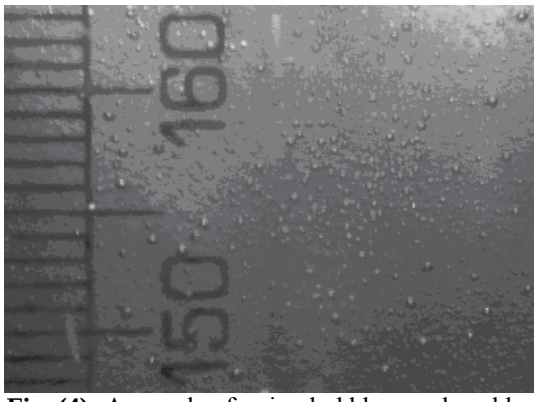

Fig. (4): A sample of microbubbles produced by the apparatus.

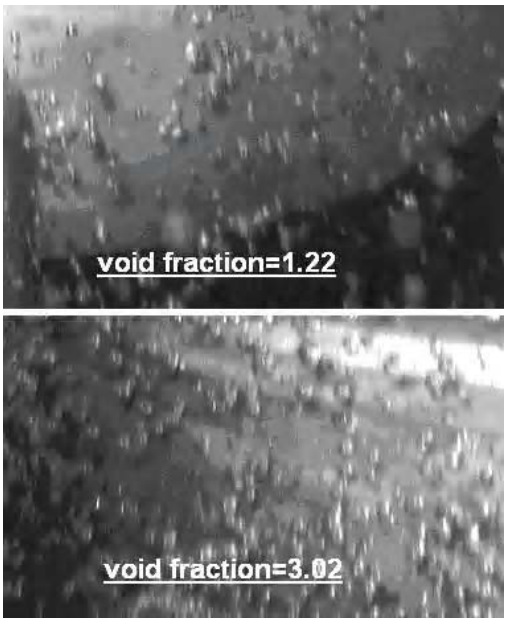

Fig. (5): Microbubbles generated from lower to upper limits of void fraction.

For void fraction more than about 4 percent, the repeatability of experiments is not guaranteed and the hub motion is discontinuous or stopped completely. This behavior was observed in all repeated tests for the void fractions from 4 to 10 percent. Figure **6** illustrates hub rotational velocity based on the water flow rate changes in various air injection rates. At each air injection rate, increasing the water flow rates caused the rotational velocity to increase. In this figure resulted in rotational velocity rise. The approximately similar behavior for each constant air flow rate indicates the same nature for both single-phase and two-phase flows, but the slope of each line changes and decreases by increasing the air flow rates. In other words, not only hub angular velocity but also its variation versus water flow rate is decreased by increasing the air flow rate. Figure **7** represents the results of hub angular velocity changes in the constant water flow rates by increasing air flow injection rates. As sketched in the figure, rotational velocity is obviously decreased by increasing air injection or void fraction.

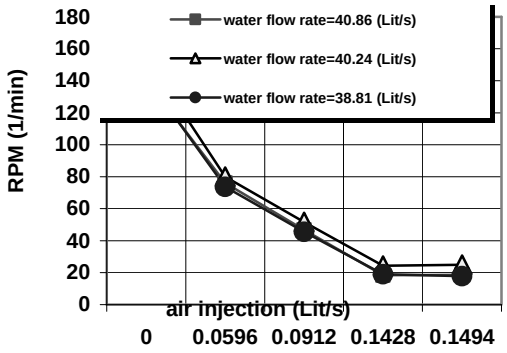

Fig. (6): Angular velocity changes by increasing air flow rate in various water flow rates.

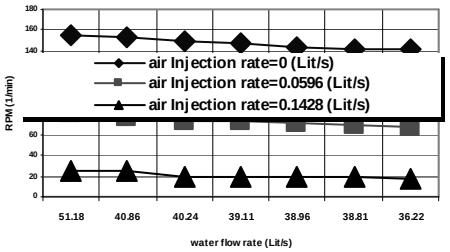

Fig. (7): Angular velocity changes by decreasing water flow rate in various air flow rates.

By normalizing the rotational velocity at each water flow rate (ω) by its maximum value in single-phase condition (ω_0), Relative Rotational Velocity (RRV) was obtained, which is one of the operating characteristics of this apparatus:

$$RRV = \frac{\omega}{\omega_0}. \qquad (2)$$

A series of repetitive tests was conducted to investigate RRV variation changes in constant void fractions. The amount of RRV decreased by increasing void fractions as shown in Fig. **8**. Since hub angular velocity is a significant parameter for the apparatus operation (microbubble-generating)

[21], this Figure can be used as a performance curve of the system.

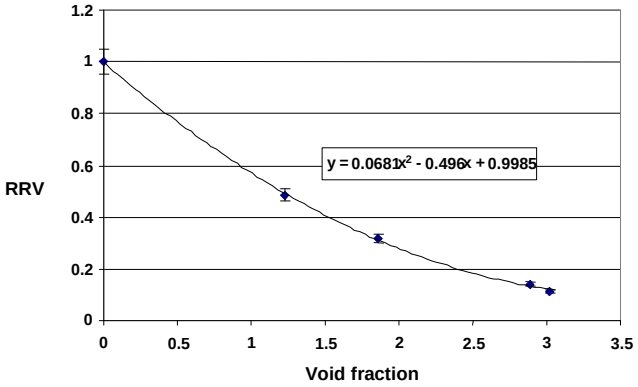

Fig. (8): Relative Rotational Velocity versus variation of void fraction.

Experimental results show a direct relationship between mean value of exerted shear stress on the rotary hub $\bar{C}_f$ and water flow rates in the examined range. Therefore, the quantities $\bar{C}_f$ and $\bar{C}_{f0}$ (mean skin friction coefficient of two- and single-phase flows, respectively) can be mutually related by hub rotational velocity. So, the percentage of the mean skin friction reduction (MSFR) can be predicted with the following equation:

$$MSFR = 1 - \frac{\omega}{\omega_0} = 1 - \frac{\omega(\bar{C}_f)}{\omega_0(\bar{C}_{f_0})} \quad . \qquad (3)$$

Table **1** represents the percentage of mean skin friction reduction by air bubble injection at each ω_0. Each row includes the relative mean skin friction reductions compared with the single-phase condition. Results in this case indicate that a small percentage of void fraction, less than 5 percent, has a strong effect on fluid motion near the wall.

The physical mechanisms and the fundamental theory of MBDR is not yet clarified completely, but several mechanisms have been suggested as playing a role in the observed drag reduction, including transport effects associated with mixture density, which Reynolds stress being diminished in the turbulent boundary layer, and turbulence energy extraction associated with vortex breakup, which diminished turbulence production associated with dilatation caused by local gradients of bubble concentration in the vicinity of the quasistreamwise vortical structures.

Apparently that, in this special case, distribution of small bubbles. near the surface of the rotary hub, affects in the shear stress produced by turbulent flow. Decrease of near wall shear stress leads to decrease of exerted force on rotary hub. This shear stress reduction appears in rotational velocity decrease of rotary hub.

Table (1): Rotational Velocity Reduction (%).

$\omega_0\,(rpm)$	Void Fraction (%)			
	1.22	1.86	2.89	3.06
155	52.00	68.00	84.00	88.00
149	54.08	69.39	86.73	90.82
144	55.10	70.41	87.76	90.82
140	53.68	69.47	87.37	91.58
Average	53.72	69.32	86.46	90.30

5- Conclusions

This experiment examined a rotary hub system used in a new apparatus to investigate the effect of air bubble injection on skin friction reduction. In this setup, tangential flows of water jets cause the rotational motion of the hub due to skin friction between the fluid flow and the hub surface. The rotational velocity of the hub was considered as an effect of skin friction and its changes were investigated in various void fractions while, in each air injection rate, some water flow rates were carried out for repeatability. Results show the tangential water jets gives rise to the rotation of the hub by constant velocity, which is proportional to water flow velocity. The results also show the small value of void fraction influence on skin friction reduction significantly. They indicate a more than 90 percent decrease in relative rotational velocity as well. It shows significant skin friction reduction by less than 4 percent of void fraction. This method is useful for avoiding the large resistant forces due to skin friction on the rotary parts of machines in a fluid.

6- References

1. Ohnari, H. "Fisheries Experiments of Cultivated Shells, Using Microbubbles Technique", J. Heat Transfer Society of Japan, Vol. 40, No. 1, pp. 2-7, 2001.
2. Serizawa, A., Inui, T., Yahiro, T., and Kawara, Z. "Laminarization of Micro-bubble Containing Milky Bubbly Flow in a Pipe", The 3rd European-Japanese Two-phase Flow Group Meeting, Certosa di Pontignano, 2003.
3. Kodama, Y., Kakugawa A., Takahashi, T., and Kawashima, H., "Experimental Study on Microbubbles and Their Applicability to Ships for Skin Friction Reduction", Int. J. Heat Fluid Flow, Vol. 21, No. 1, pp. 582-588, 2000.
4. Deutch, S., Money, M., Fontaine, A.A., and Petrie, H. "Microbubble Drag Reduction in Rough Walled Turbulent Boundary Layers with Comparison against Polymer Drag Reduction",

Experiments in Fluids, Vol. 37, No. 2, pp. 731-744, 2004.
5. McCormick, M.E. and Bhattacharyya, R. "Drag Reduction on a Submersible Hull by Electrolysis, Nav. Eng. J., Vol. 85, No. 2, pp. 11-16, 1973.
6. Hassan, Y.A., and Torres, C.C.G. "Investigation of Drag Reduction Mechanism by Microbubble Injection within a Channel Boundary Layer, Using Particle Tracking Velocimetry", Nuclear Eng. and Tech., Vol. 38, No. 2, pp. 763-779, 2006.
7. Latorre, R., Miller, A., and Philips R. "Micro-bubble Resistance Reduction on a Model SES Catamaran", Ocean Eng., Vol. 30, No. 1, pp. 2297-2309, 2003.
8. Sanders, W.C., Winkel, E.S., Dowling, D.R., Perlin, M., and Ceccio, S.L. "Bubble Friction Drag Reduction in a High-Reynolds-Number Flat-Plate Turbulent Boundary Layer", J. Fluid Mech., Vol. 552, No. 1, pp. 353-380, 2006.
9. Chanson, H. "Drag Reduction in Open Channel Flow by Aeration and Suspended Load", J. Hydraulic Research, Vol. 32, No. 1, pp. 87-101, 1994.
10. Fujiwara, A., Minato, D., and Hishida, K. "Effect of Bubble Diameter on Modification of Turbulence in an Upward Pipe Flow", Int. J. Heat and Fluid Flow, Vol. 25, No. 1, pp. 481-488, 2004.
11. Murai, Y., Oiwa, H., and Takeda, Y. "Bubble Behavior in a Vertical Taylor-Couette Flow, J. Physics, Conf. Series, Vol. 14, No. 1, pp. 143-156, 2005.
12. Villafuerte, J.O. and Hassan, Y.A "Investigation of Microbubble Boundary Layer, Using Particle Tracking Velocimetry", J. Fluids Eng., Vol. 128, No. 4, pp. 507-519, 2006.
13. Wu, S.J., Hsu, C.H., and Lin, T.T. "Model Test of the Surface and Submerged Vehicles with the Micro-bubble Drag Reduction", Ocean Eng., Vol. 34, No. 1, pp. 83-93, 2007.
14. Murai, Y., Fukuda, H., Oishi, Y., Kodama, Y., and Yamamoto, F. "Skin Friction Reduction by Large Air Bubbles in a Horizontal Channel Flow", Int. J. Multiphase Flow, Vol. 33, No. 3, pp. 147-163, 2007.
15. Shen, X., Ceccio, S.L., and Perlin, M. "Influence of Bubble Size on Micro-Bubble Drag Reduction", Experiments in Fluids, Vol. 41, No. 33, pp. 415-424, 2006.
16. Lu, J., Fernández, A., and Tryggvason, G. "The Effect of Bubbles on the Wall Drag in a Turbulent Channel Flow", Physics of Fluids, Vol. 17, No. 1, 2005.
17. Kitagawa, A., Hishida, K., and Kodama, Y. "Flow Structure of Microbubble-laden Turbulent Channel Flow Measured by PIV Combined with the Shadow Image Technique", Experiments in Fluids, Vol. 38, No. 4, pp. 466-475, 2005.
18. Ferrante, A. and Elghobashi, S.R., Number Effect on Drag Reduction in a Microbubble-laden Spatially Developing Turbulent Boundary Layer", J. Fluid Mech., Vol. 543, No. 24, pp. 93-106, 2005.
19. Kunz, R.F., Gibeling, H.J., Maxey, M.R., Tryggvason, G., Fontaine, A.A., Petrie, H., and Ceccio, S.L. "Validation of Two-Fluid Eulerian CFD Modeling for Microbubble Drag Reduction Across a Wide Range of Reynolds Numbers", Transactions of the ASME, pp. 66-79, 2007.
20. Skudarnov, P.V. and Lin, C.X. "Drag Reduction by Gas Injection into Turbulent Boundary Layer: Density Ratio Effect", Int. J. Heat and Fluid Flow, Vol. 27, No. 2, pp. 436-444, 2006.
21. Nouri, N.M., Maghsoudi, E., Sarreshtehdari, A., and Yahyaei, M. "Microbubble Generation, Using High Turbulent Intensity Flow", FEDSM 2007, The 5th Joint ASME/JSME Fluids Eng. Conf., San Diego, California, USA, 2007.